# CFD-BASED NUMERICAL SIMULATION OF SELF-PROPULSION FOR JAPAN BULK CARRIER

**Jianwei Wu(Shanghai Jiao Tong University, State Key Laboratory of Ocean Engineering, Collaborative Innovation Center for Advanced Ship and Deep-Sea Exploration, China)**
**Chonghong Yin(Shanghai Jiao Tong University, State Key Laboratory of Ocean Engineering, Collaborative Innovation Center for Advanced Ship and Deep-Sea Exploration, China)**
**Tao Sun(Shanghai Jiao Tong University, State Key Laboratory of Ocean Engineering, Collaborative Innovation Center for Advanced Ship and Deep-Sea Exploration, China)**
**Decheng Wan* (Shanghai Jiao Tong University, State Key Laboratory of Ocean Engineering, Collaborative Innovation Center for Advanced Ship and Deep-Sea Exploration, China)**
***Corresponding author: dcwan@sjtu.edu.cn**

## 1. ABSTRACT

Self-propulsion movements of JAPAN Bulk Carrier is investigated numerically using overset grid method in present work. Dynamic overset grid is such a method which allows different part of model to move independently. Accordingly, the propeller can keep rotating when ship hull is advancing along a straight path during the computation. Computations in this work are performed with the solver naoe-FOAM-os-SJTU, which is developed and based on the open source CFD tool OpenFOAM to solve hydrodynamic problems of ships and ocean engineering, and the overset grid method is implemented in it. In order to get the self-propulsion point, we utilize a speed controller to keep adjusting the rotational speed of the direct discretized propeller automatically until the ship hull reaches the target speed under a SFC (Skin Friction Correction) force and the thrust, and the effect of free surface is taken into consideration here. Self-propulsion point and self-propulsion factors are analyzed and compared with experimental measurements.

KEY WORDS: Overset grid, CFD, Self-propulsion, discretized propeller, naoe-FOAM-os-SJTU, free surface

## 2. INTRODUCTION

Self-propulsion test is crucially important for ship design, especially powering design. On the one hand, it can be used in performance estimation of full-scale ship, on the other hand, it can evaluate the matching level among ship hull, propeller and marine main engine. As we known, there are two methods to carry out self-propulsion test, England Method and Mainland Method. The former is much easier to implement so it is usually applied in model test. To get the self-propulsion point under target speed, the propeller have to work under several specific rotational speeds while the ship hull, fixed at the towing, is advancing at a constant speed. When the self-propulsion point is reached, the towing force is strictly equal to SFC (Skin Friction Correction) force. Eventually, we can get the self propulsion point by interpolating on ship model self-propulsion curve. With the development of CFD, it is probable to realize the Mainland Method. During the computation, SFC force is exerted on ship hull constantly, and the rotational speed of the propeller is controlled with a PI speed controller. The objective is to make the hull reach specific speed rapidly and automatically. Finally, we can get the self-propulsion point result by monitor the final motion states of hull and propeller.

In the past decades, computational fluid dynamics (CFD) has become one of the most popular research tools to solve hydrodynamic problems. Not only can it evaluate the hydrodynamic characters of ship and ocean engineering structures, but also CFD provides much detail information of the flow field. For the self-propulsion simulation, the implement of overset grid technology is a curial step. Every dynamic object, including hull and propeller, is generated grids independently at the beginning, then they are nested in the same background grids and some mesh processes are adopted here too. Within the overset region, flow field information is exchanged through interpolation method. Overset grid method breaks the restrictions of the mesh topology among different objects and allows grids to move independently within the computational domain. In this present work, the interaction between hull and propeller is simulated by CFD tool equipped with overset grid approach.

The simulations of self-propulsion test are reported in the literature. Carrica *et all.* made self-propulsion computations using a speed controller and a discretized propeller with dynamic overset grids for three ship hulls, including the single-propeller KVLCC1 tanker appended with a rudder, the twin propeller fully appended surface combatant model DTMB 5613, and the KCS container ship without a rudder, and the results were compared with experimental data obtained at the model scale. Shen *et all.* implemented overset grid approach in the open source code OpenFOAM, Ship motions of KCS in head waves with and without rotating propeller were investigated using overset grid method in the paper, and this work validated the overset code in OpenFOAM and demonstrated the capability of overset grid approach when solving complex problems. Yang *et all.* used CFD method to simulate the unsteady viscous-flow for containership KCS with propeller and tanker ship KVLCC2 with propeller and rudder, in which the simulations of hull/propeller/rudder interaction were carried by adding momentum source, MRF method and sliding mesh method respectively. The merit of each method was also discussed here.

In this paper, self-propulsion test of JBC is simulated and investigated, it is notable that the effect of free surface and discretized propeller are taken into consideration. The computations in present work are performed with naoeFoam-os-SJTU solver, a CFD tool developed basing on open source code OpenFOAM and equipped with overset grid technique. We also utilize SUGGAR program to generate the domain connectivity information (DCI) for the overset grid interpolation.

## 3. NUMERICAL METHODS

### 3.1 Governing equations

In this paper, the continuity equation and the Reynolds averaged Navier-Stokes (RANS) equations are adopted as the governing equations, which is presented as follows:

$$\nabla\cdot U=0 \tag{1}$$

$$\frac{\partial\rho U}{\partial t}+\nabla\cdot(\rho(U-U_g)U)=-\nabla p_d-g\cdot x\nabla\rho +\nabla\cdot(\mu_{eff}\nabla U)+(\nabla U)\cdot\nabla\mu_{eff}+f_\sigma+f_s \tag{2}$$

where, $U$ stands for the velocity field; $U_g$ means the velocity of grid nodes; $p_d$ is dynamic pressure，which can be obtained by subtracting the hydrostatic component from the total pressure; $\rho$ is mixed density of the two phases, water and air; $g$ represents the gravitational acceleration vector; $\mu_{eff}$ is the effective dynamic viscosity, and is equal to $\rho(\nu+\nu_t)$, where $\nu$ is kinematic viscosity coefficient and $\nu_t$ is eddy viscosity; $f_\sigma$ is the surface tension term, which impacts the free surface. $f_s$ is a source term, added to generate the sponge layer for wave damping.

### 3.2 Capture of free surface

In this paper, the volume of fluid (VOF) method with artificial bounded compression techniques is used to capture the free surface of the two-phase flow. The transport equation is formulated as follows:

$$\frac{\partial\alpha}{\partial t}+\nabla\cdot[(U-U_g)\alpha]+\nabla\cdot[U_r(1-\alpha)\alpha]=0 \tag{3}$$

in which the α represents the volume of fraction function, which is defined as:

$$\alpha(x,t)=\begin{cases}\alpha=0 & \text{air}\\ \alpha=1 & \text{water}\\ 0<\alpha<1 & \text{interface}\end{cases} \tag{4}$$

in equation (3) $U_r$ is the velocity field compressing the interface, and can be obtained as the follow expression:

$$U_{r,f}=n_f\min\left\{C_\alpha\frac{|\phi|}{|S_f|},\max\left(\frac{|\phi|}{|S_f|}\right)\right\} \tag{5}$$

where $\varphi$ is face volume flux; $C_\alpha$ is a compression coefficient controlling the magnitude of compression, in this paper it is chosen to be 1.0; $S_f$ is the normal vector of a cell face and its magnitude equals to the area of the cell face. $n_f$ is the unit normal vector on interface.

### 3.3 Motion mode

A fully 6DOF module with hierarchy of bodies is implemented in naoeFoam-os-SJTU solver. Two coordinates are introduced here, including earth-fixed system and ship-fixed system. The forces and moments exerted on ship hull and propeller are computed in earth-fixed system, and then they should be projected to ship-fixed system to solve 6DOF motion equations, eventually, the displacements are switched to earth-fixed system. Accordingly, the ship model is allowed to move independently in the computational domain. The movement mode of hierarchal objects is developed as an extension of 6DOF module to handle complex movement problems. The first level is the background grids, the second level is the ship hull grids, and the third level is the propeller grids. The principle is the lowest level moves first. Hence, the propeller grids are rotated around its axis first, then the position and orientation of the ship hull grids at the next time step are calculated followed, and the last step is to translate or rotate the background grids in terms of user's presets. Additionally, this method is also effective for conditions like a ship hull with several appendages.

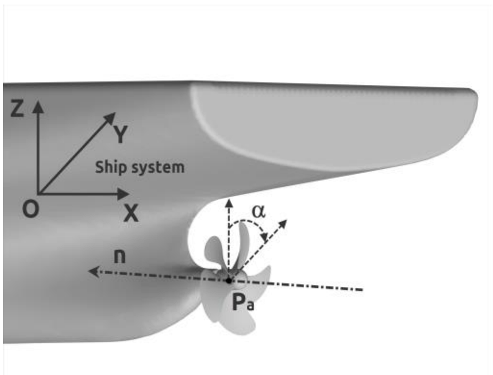


Fig.1 Sketch of the ship hull and the rotating propeller

### 3.4 Discretization scheme and decoupling method

We utilize the finite volume method (FVM) proposed by Hino in 1993 to discretize the RANS equations and VOF transport equation. We discrete the computational domain into a number of cells and every control volume surrounding a node point, at which the field information is stored. Furthermore, the PISO (pressure implicit split operator) algorithm is used to solve the coupled equation of velocity and pressure. Besides, the SST k-ω turbulence model is employed as the turbulence model in present work.

## 4. GEOMETRY , GRIDS AND CONDITONS

### 4.1 Geometry

JAPAN Bulk Carrier (JBC) is a capesize bulk carrier, National Maritime Research Institute (NMRI), Yokohoma University, Ship Building Research Centre of Japan (SRC) are jointly involved in the design of it. Towing tank experiments including resistance tests, self-propulsion tests and PIV measurements of stern flow fields are planned at NMRI, SRC and Osaka University. Main particulars of JBC for both of full and model scale are listed in Table 1, and the 3D model of hull is shown in Fig. 2.

Table 1 Hull data of JBC

| Main particulars | | Full scale | Model scale |
|---|---|---|---|
| Length between perpendiculars | $L_{PP}$ (m) | 280 | 7 |
| Length of waterline | $L_{WL}$ (m) | 285 | 7.125 |
| Maximum beam of waterline | $B_{WL}$ (m) | 45 | 1.125 |
| Depth | D (m) | 25 | 0.625 |
| Draft | T (m) | 16.5 | 0.4125 |
| Displacement volume | $\nabla$ ($m^3$) | 178369.9 | 2.7870 |
| Wetted surface area | S ($m^2$) | 19556.1 | 12.2226 |
| Block coefficient | $C_B$ | 0.858 | 0.858 |
| Midship section coefficient | $C_M$ | 0.9981 | 0.9981 |
| LCB (%$L_{PP}$), fwd+ | LCB | 2.5475 | 2.5475 |

Fig.2 Geometry of JBC hull

The ship is fitted with a five-blades propeller. The longitudinal location of the propeller center is $x/L_{PP}$ = 0.9857, and the vertical location of the propeller center is $-z/L_{PP}$ = -0.04042. The propeller diameter in model scale is 0.203m. Fig. 3 shows the 3D model of propeller.

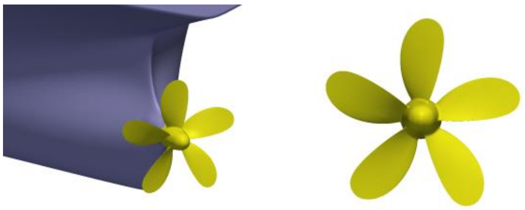

Fig.3 Geometry of propeller

### 4.2 Grids and domain

To implement overset grid approach, grids for every dynamic object such as hull and propeller are generated independently, then they are nested in the background grids, and some mesh processes are adopted here before computations. The amount of grids for every part is listed in Table 2.

Table 2 Amount of grids for every part

| Part | Hull | Propeller | Background | Total |
|---|---|---|---|---|
| Amount | $1.42\times10^6$ | $1.90\times10^6$ | $1.41\times10^6$ | $4.73\times10^6$ |

SnappyHexMesh, a mesh generating tool provided by OpenFOAM is applied to generate grids in this paper. The calculation domain is $-1.0L_{pp}<x<4.0L_{pp}$, $-1.5L_{pp}<y<1.5L_{pp}$, $-1.0L_{pp}<z<1.0L_{pp}$. Some details of meshes are illustrated in Fig. 4, and the boundary conditions for computation are shown in Fig. 5.

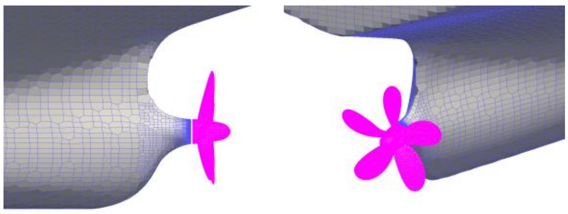

Fig.4 Mesh used for numerical computation

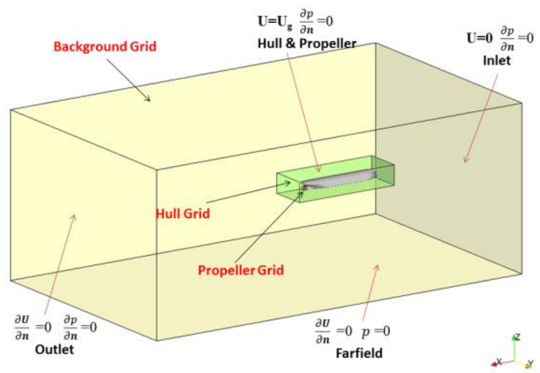


Fig.5 Boundary conditions for numerical computation

### 4.3 Conditions

In this computation, the service speed of JBC is 14.5kn, and the corresponding Froude number is 0.142. The JBC hull, propelled by propeller, is advancing at a constant and specific speed in calm water, and an artificial force named SFC (Skin Friction Correction) is exerted on ship model to obtain the self-propulsion point of ship under tank conditions.

## 5. RESULTS

The computations for self-propulsion are started with predicting the drag of JBC hull without any appendages, and the open-water performance of propeller is studied followed. These results will be needed later in the analysis of propulsion factors, and these numerical calculations are also used to verify the feasibility and validity of overset grid technique.

There are two points to clarify before we present the results. A PI speed controller is applied to control the propeller RPS. The error is defined as the difference between the instantaneous ship speed and the target speed, and the instantaneous RPS can be obtained based on equation (7) .

$$e = U_{\text{target}} - U_{\text{ship}} \qquad (6)$$

$$n = Pe + I\int_0^t e\,dt \qquad (7)$$

where P and I are the proportional and integral constants of the controller.

During the simulation of self-propulsion test, an artificial force named SFC (Skin Friction Correction) is exerted on ship hull. It is used to correct the difference of fraction resistance coefficient between full-scale and model-scale ship. The SFC can be estimated from equation (8).

$$\mathrm{SFC} = \{(1+\mathrm{k})(C_{F0M} - C_{F0S}) - \Delta C_F\} \times \frac{1}{2}\rho U_0^2 S_W \qquad (8)$$

where $C_{F0M}$ and $C_{F0S}$ can be obtained from the 1957-ITTC formula; $U_0$ is the reference velocity; $S_W$ is the static wetted area; 1+k is shape factor; $\Delta C_F$ is the roughness allowance can be estimated by equation (9):

$$\Delta C_F = 0.044 \times \left[\left(\frac{k_s}{L_{pp}}\right)^{1/3} - 10\,\mathrm{Re}^{-1/3}\right] + 1.25 \times 10^{-4} \qquad (9)$$

So, we get equation (10), where $R_{T(SP)}$ is the hull resistance of JBC under self-propulsion condition; $T$ is the propeller thrust; the $SFC$ is as descriptions above.

$$T = R_{T(SP)} - SFC \qquad (10)$$

### 5.1 Simulation of resistance test

The computational results of resistance and motions for bare hull without any appendages are listed in Table 3.

Table 3 Results of resistance test for JBC

| Parameters | CFD | EFD | ERROR (%) |
|---|---|---|---|
| $C_p(\times 10^{-3})$ | 1.439 | - | - |
| $C_v(\times 10^{-3})$ | 2.737 | - | - |
| $C_t(\times 10^{-3})$ | 4.176 | 4.289 | 2.62 |
| *Sinkage/m* | -0.08421 | -0.086 | 2.08 |
| Parameters | CFD | EFD | ERROR(%) |
| *Trim /°* | -0.1711 | -0.18 | 4.93 |

### 5.2 Simulation of propeller open-water test

The propeller open-water test is simulated in this section in order to get the open-water curve and evaluate the ability of the solver as well. The computations are performed using the computation towing tank procedures of Xing et al., where a small acceleration was imposed on the propeller to cover a continuous and wide range of velocities in a single run. The boundary conditions of the single-run case are displayed in Fig. 6, and the open-water curve is showed in Fig. 7. Fig. 8 shows the isosurfaces of Q=400 for four different advance coefficients 0.16, 0.32, 0.48 and 0.64 in single-run computation.

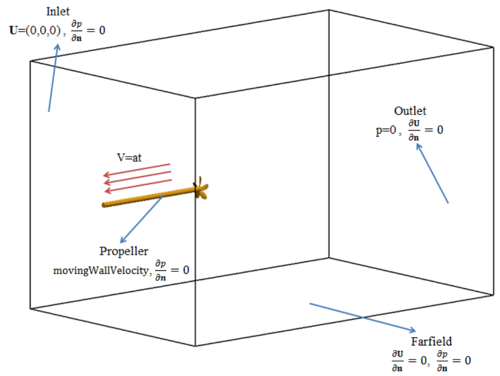


Fig. 6. Boundary conditions

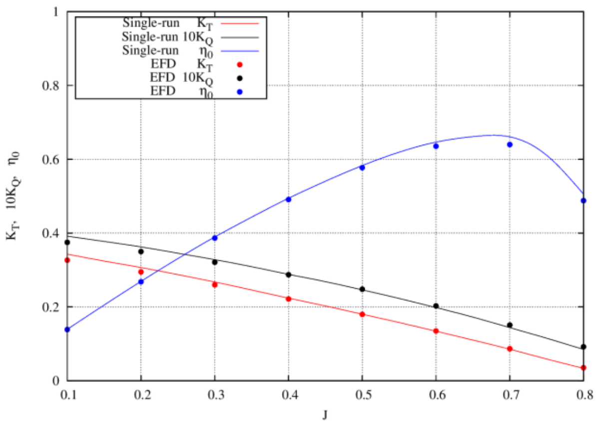


Fig. 7. Propeller open-water curve

| | | | |
|---|---|---|---|
| $K_T$ | 0.2226 | 0.217 | -2.55 |
| $K_Q$ | 0.0287 | 0.0279 | -2.76 |

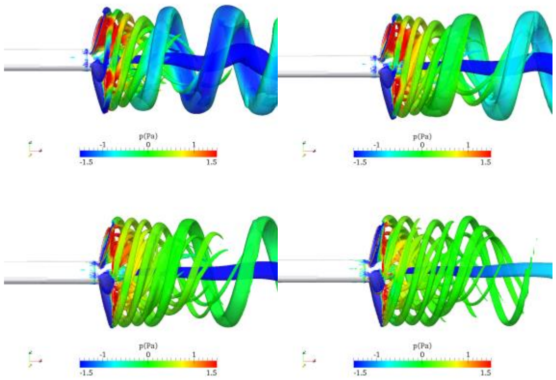

Fig. 8. Isosurfaces of Q=400 for J = 0.16, 0.32, 0.48

The calculated results are in good agreement with experimental results. This lays the foundation for the later simulation of self-propulsion test.

## 5.3 Simulation of self-propulsion test

In this part, self-propulsion computations with specified SFC force are performed. The JBC hull is fitted with a five-bladed propeller denominated MP687. The RPS of the propeller is to be controlled by using a PI controller in terms of the instantaneous speed and instantaneous force exerted on ship hull.

In self-propulsion case, SFC force is equal to 18.1 N, the time step is $2.5\times10^{-4}$s , corresponding to it in propeller open-water case, the target speed for ship hull is 1.179m/s (Fr = 0.142), the proportional and integral controller constants are set to P=I=800. Self-propulsion point and self-propulsion factors are compared with experimental data in Table 4 and Table 5. The self-propulsion factors are obtained by using the equal thrust method recommended by ITTC, and the experimental measurements of open-water curve for MP687 propeller provided by NMRI are applied here.

Table 4 Results of the self-propulsion point for JBC

| | CFD | EFD | ERROR(%) |
|---|---|---|---|
| *Sinkage (m)* | -0.00686 | - | - |
| *Trim (°)* | -0.0921 | - | - |
| $C_t(\times10^{-3})$ | 4.607 | 4.811 | 4.24 |
| *U (m/s)* | 1.179 | 1.179 | 0 |
| *RPS (r/s)* | 7.682 | 7.8 | 1.51 |
| *SFC (N)* | 18.2 | 18.2 | 0 |
| *T (N)* | 22.26 | - | - |
| *Q (m·N)* | 0.5821 | - | - |

Table 5 Results of the self-propulsion factors for JBC

| | CFD | EFD | ERROR(%) |
|---|---|---|---|
| $C_t$ | 0.00461 | 0.00481 | 4.238 |
| $K_T$ | 0.22255 | 0.21700 | -2.558 |
| $10K_Q$ | 0.28671 | 0.27900 | -2.762 |
| $10K_{Q0}$ | 0.28860 | 0.28342 | -1.828 |
| *1-t* | 0.93095 | 0.89150 | -4.426 |
| *1-w* | 0.52678 | 0.54830 | 3.924 |
| $\eta_0$ | 0.48953 | 0.49810 | 1.720 |
| $\eta_R$ | 1.00659 | 1.01583 | 0.909 |
| *J* | 0.39827 | 0.40826 | 2.449 |
| *n* | 7.682 | 7.8 | 1.513 |
| $\eta_H$ | 0.87083 | 0.82270 | -5.851 |

In Table 5, *t* is the thrust deduction coefficient; *w* is the wake fraction coefficient; $\eta_0$ is the open water propeller efficiency; $\eta_R$ is the relative rotative efficiency; $\eta_H$ is the hull efficiency defined as $\eta_H = (1\text{-}t)/(1\text{-}w)\times\eta_0\times\eta_R$. The $K_{Q0}$ is obtained from open-water curves by using the equal thrust method.

The pressure distribution on ship hull and propeller is presented in Fig. 9. The free surface around ship hull is presented in Fig. 10. The vortex structures around stern are presented in Fig. 11 where isosurfaces of Q=100 colored with $U_x$ are employed for vortex identification.

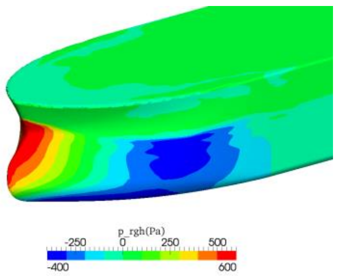


(a) bow

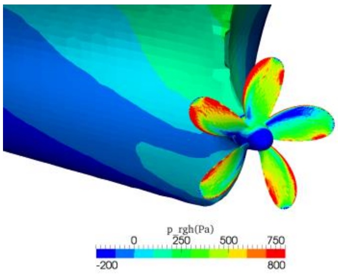


(b) stern

Fig. 9. Pressure distribution

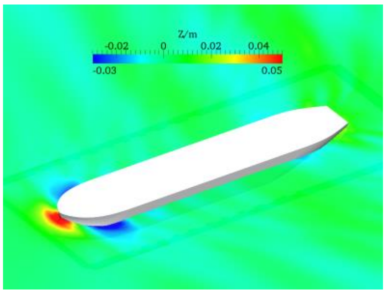


Fig. 10. Free surface

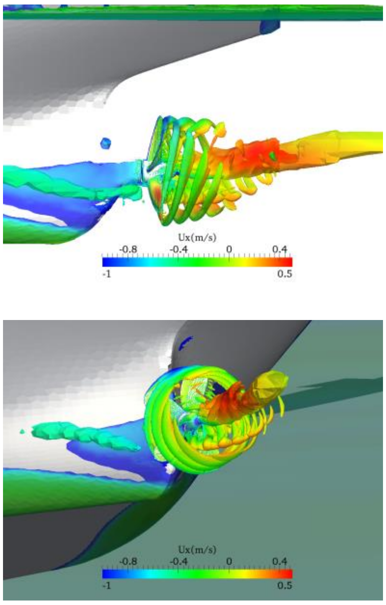


Fig. 11. Isosurfaces of Q=100 colored with Ux

## 6. CONCLUSIONS

In this paper, a numerical simulation of self-propulsion is carried out for JAPAN Bulk Carrier by using overset grid method. Dynamic overset grid is such a method which allows the propeller to keep rotating while ship hull is advancing during the computation, and the RPS of the propeller is to be adjusted by using a PI controller in terms of the instantaneous speed and instantaneous force exerted on ship hull. All of the computations in this work are performed with the solver naoe-FOAM-os-SJTU, which is developed and based on the open source CFD tool OpenFOAM to solve hydrodynamic problems of ships and ocean engineering, and the overset grid method is implemented in it.

The resistance test and the propeller open-water test are investigated numerically firstly for getting both of the resistance performance for hull and the open water performance for propeller, which will be needed in the analysis of propulsion factors later. These results have a good agreement with the experimental measurements, so it lays the foundation for the later simulation of self-propulsion test. In the self-propulsion case, SFC force is exerted on ship hull as a correction to the difference of fraction resistance coefficient between full-scale and model-scale ship. The equal thrust method recommended by ITTC is conducted here. The self-propulsion point and self-propulsion factors are obtained and compared with experimental measurements eventually, as shown in Table 4 and Table 5, the relative errors are mostly less than 5%.

The effectiveness and feasibility of naoe-FOAM-os-SJTU solver is validated, and it is proved to be reliable to solve complex problem, such as propeller-hull interaction issue. In the next step, more validation cases including free maneuvering and seakeeping will be performed.

## REFERENCES

Carrica, P.M., Castro, A.M. and Stern, F., (2010), “Self-propulsion computations using a speed controller and a discretized propeller with dynamic overset grids”, *Journal of Marine Science and Technology*, 15(4):316-330.

Shen, Z.R., Carrica, P.M. and Wan, D.C., (2014), “Ship motions of KCS in head waves with rotating propeller using overset grid method”. In the Proceedings of the 33rd International Conference on Ocean, Offshore and Arctic Engineering. San Francisco, California, USA.

Yang, C.L., Zhu, R.C., Miao, G.P., Fan, J., Li, Y.L., (2011), “CFD-based numerical simulation of hull propeller rudder interaction”, *Chinese Journal of Hydrodynamics*, 26(6): 667–673.

ITTC., (2002), “Testing and Extrapolation Methods Propulsion, Performance Propulsion Test (Recommended Procedures and Guidelines) ”. 7.5-02-03-01.1.

Noack, R.W., (2005), “SUGGAR: a general capability for moving body overset grid assembly”. 17th AIAA Computational Fluid Dynamics Conference, Toronto, Ontario, Canada.

Hino, T., (1987), “Numerical simulation of a viscous flow with a free surface around a ship model”. *Journal of the Society of Naval Architects of Japan*, 161: 1–9.

Issa, R.I., (1986), “Solution of the implicitly discretised fluid flow equations by operator-splitting”. *Journal of*

*Computational Physics*, 62(1): 40–65.